Molecular Phylogenetics and Evolution 58 (2011) 478–491

Contents lists available at ScienceDirect

Molecular Phylogenetics and Evolution

journal homepage: www.elsevier.com/locate/ympev

Comparative population genetics and phylogeography of two lacertid lizards (*Eremias argus* and *E. brenchleyi*) from China

Qun Zhao [a,b], Hong-Xia Liu [a], Lai-Gao Luo [b], Xiang Ji [a,*]

[a] Jiangsu Key Laboratory for Biodiversity and Biotechnology, College of Life Sciences, Nanjing Normal University, Nanjing 210046, Jiangsu, China
[b] Hangzhou Key Laboratory for Animal Adaptation and Evolution, School of Life Sciences, Hangzhou Normal University, Hangzhou 310036, Zhejiang, China

ARTICLE INFO

Article history:
Received 30 July 2010
Revised 27 December 2010
Accepted 28 December 2010
Available online 6 January 2011

Keywords:
Eremias lizards
Mitochondrial DNA
Cytochrome *b*
Phylogeography
Vicariance
Population genetics

ABSTRACT

Eremias argus and *Eremias brenchleyi* are lacertid lizards that are sympatric throughout the distribution of *E. brenchleyi*. We sequenced partial mitochondrial DNA from cytochrome (cyt) *b* gene for 106 individuals of *E. argus* from nine localities, and for 45 individuals of *E. brenchleyi* from five localities, in central and northern parts of North China. We determined 53 cyt *b* haplotypes from the *E. argus* samples, and 27 cyt *b* haplotypes from the *E. brenchleyi* samples. Only *E. brenchleyi* had followed a stepping-stone model of dispersal. Partitioned Bayesian phylogenetic analysis reveals that *E. argus* and *E. brenchleyi* are reciprocally monophyletic, and the divergence time between the two species was dated to about 4.1 ± 1.2 million years ago. Geographical structuring of haplotypes is more significant in *E. brenchleyi* than in *E. argus*. Haplotypes of *E. brenchleyi* could be divided into four groups by the Yellow River and Taihang Mountains. Within-population genetic diversity indices are correlated neither with latitude nor with longitude. We calculated significant among-population structure for both species (*E. argus*: $\Phi_{ST} = 0.608$, $P < 0.001$; *E. brenchleyi*: $\Phi_{ST} = 0.925$, $P < 0.001$). *Eremias brenchleyi* has four independent management units, while *E. argus* has a more homogeneous genetic structure across its range. Our data show that: (1) the pattern seen in North American and European species that southern populations have higher genetic diversity as consequence of post-glaciation dispersal is absent in the two Chinese lizards; (2) the Yellow River and Taihang Mountains may have acted as important barriers to gene flow only in *E. brenchleyi*; and (3) genetic structure differs between the two lizards that differ in habitat preference and dispersal ability.

1. Introduction

Many factors (e.g. geological, ecological, and genetic) interact to form population genetic patterns of species (Wares and Turner, 2003; Byrne, 2008). Climatic changes, which were the major environmental changes during Pleistocene glacial–interglacial cycles, have played a dramatic role in shaping genetic diversity of species (Avise, 2000; Hewitt, 1996, 1999, 2000, 2004), and the severe climatic oscillations produced great changes in species distributions (Hewitt, 2000). Knowledge of phylogeography of terrestrial species is considerable for taxa from North America and Europe, but relatively little for Asian species. In North American and European regions that were glaciated, widespread terrestrial species expanded from southern refugia at the end of the Pleistocene, thus exhibiting less geographically structured genetic diversity in the north (Hewitt, 1996, 1999, 2000).

Compared with North America and Europe, most of East Asia was never covered by ice sheets during the Pleistocene (Williams et al., 1998). On the Tibetan Plateau, however, the area of the ancient ice cap during the last glacial maximum exceeded 350,000 km^2, marked by piedmont glaciers, ice caps and trellis valley glaciers in many high peak regions (Li et al., 1991). The present fauna on the plateau is probably from post-Pleistocene migrations (Zhang and Zheng, 1981). The geography of China associated with the collision of the Indian subcontinent with the mainland of Asia is tectonically active, highly dissected, and elevated, which has made the region one of the most important global Pleistocene refugia for lineages that evolved prior to the late Tertiary and Quaternary glaciations (Axelrod et al., 1996). Most of China has never been covered by ice sheets and had a relatively mild Pleistocene climate, and thus differs from Europe and North America (Weaver et al., 1998; Ju et al., 2007). Nonetheless, environmental changes associated with Pleistocene climatic oscillations have influenced the distribution and evolution of many plants and animals in China (e.g. Axelrod et al., 1996; Zhang et al., 2005; Meng et al., 2008; Zhang et al., 2008a; Li et al., 2009).

Recent phylogeographic studies reveal remarkably different patterns of genetic diversity among co-distributed species, showing that climatic change is just one among many factors that interact to shape population genetic patterns (e.g. Hewitt, 2004; Gómez and Lunt, 2007; Byrne, 2008; Elderkin et al., 2008). Climatic changes

* Corresponding author. Fax: +86 25 85891526.
E-mail address: xji@mail.hz.zj.cn (X. Ji).

1055-7903/$ - see front matter © 2011 Elsevier Inc. All rights reserved.
doi:10.1016/j.ympev.2010.12.017

interact with mountains and rivers to fragment many terrestrial species, leading to multiplication of species (Zhang et al., 2008b; Jin et al., 2008). Other factors such as habitat preference and dispersal ability also affect genetic relationships within and among populations (Bohonak, 1999; Bilton et al., 2001; Elderkin et al., 2008). It has been known that unique dispersal events may produce contrasting phylogeographies for co-distributed species (Page, 1994), and that dispersal is a key factor for the persistence of metapopulations in fragmented landscapes (Hanski, 1998; Thomas, 2000).

The Mongolian racerunner *Eremias argus* and the Ordos racerunner *Eremias brenchleyi* studied herein both are small, oviparous, and heliothermic lacertid lizards that are sympatric throughout the distribution of *E. argus* in the central and northern parts of China (Chen, 1991). The two lizards can coexist primarily because they use different microhabitats not because they differ so much in the resource axes of diet and time (Zhao, 1999). In this study, we use partial mtDNA sequences from cytochrome (cyt) *b* gene to study the genetic diversity, the population-genetic structure, population demographic history, and phylogeography of the two lizards. We address three main questions: (1) Can the pattern seen in North American and European species that southern populations have higher genetic diversity as consequence of post-glaciation dispersal be observed in the two Chinese lizards? (2) May important rivers and mountains such as the Yellow River and Taihang Mountains within the distribution of the two lizards have acted as barriers to gene flow? (3) Does genetic structure differ between lizards that differ in habitat preference and dispersal ability?

2. Materials and methods

2.1. Locations

Lizards of *E. argus* were sampled from two regions, one in the south of the Yellow River (SYR) and the other in the north of the river (NYR). From SYR, one population each was collected in Chuzhou (CZ), Chang'an (CA), and Etuoke (ETK). From NYR, one population each was collected in Jiyuan (JY), Gonghe (GH), Handan (HD), Yangquan (YQ), Xinhe (XH), and Harbin (HRB) (Fig. 1A).

Lizards of *E. brenchleyi* were also sampled from the two regions. From SYR, one population each was collected in Xuzhou (XZ) and Taishan (TS). From NYR, one population each was collected in JY, HD, and YQ (Fig. 1B).

2.2. Sampling

We collected 106 individuals of *E. argus* from nine localities (Fig. 1A), and 45 individuals of *E. brenchleyi* from five localities (Fig. 1B). The geographical position of each sampling locality was marked using a global positioning system. Appendices A and B and Table 1 show the number of individuals collected at each locality and other information used in this study. All sequences from the two species in this study and six sequences from three congeneric species (*E. velox*, *E. montanus*, and *E. nigrolateralis*) were used as ingroups for the phylogenetic analysis of the mtDNA. *Mesalina brevirostris* and *Ophisops elegans* (Fu, 1998, 2000; Hipsley et al., 2009) were used as outgroup taxa for our phylogenetic analysis. New sequences for *E. argus* and *E. brenchleyi* were produced in the present study, while all other sequences were retrieved from GenBank.

2.3. Molecular data

Lizards of both species were treated similarly for DNA analysis. Tail tissue was sampled from each individual and stored in −80 °C, and whole genomic DNA was extracted from tail samples using standard phenol–chloroform extraction and ethanol precipitation protocols (Palumbi, 1996).

We used the primers L14910 (5′-GAC CTG TGA TMT GAA AAA CCA YCG TTG T-3′) and H16064 (5′-CTT TGG TTT ACA AGA ACA ATG CTT TA-3′) to amplify a partial DNA fragment of the cyt *b* gene (Burbrink et al., 2000). Polymerase chain reaction (PCR) was performed in 100 μl volumes, using a hot start method; PCR conditions were 7 min at 94 °C; 40 cycles of 40 s at 94 °C, 30 s at 46 °C, and 1 min at 72 °C; and 7 min at 72 °C. For cycle sequencing, we used primers L14761 (5′-MTC HAA CAA CCC AAY MGG-3′), H14892 (5′-TGC NGG KGT RAA KTT TTC-3′) and H15149 (5′-CCC TCA GAA TGA TAT TTG TCC TCA-3′). After removing primers and unincorporated nucleotides with a spin column containing Sepacry S-400 (Amersham Bioscience AB, Uppsala, Sweden), the purified amplified products were sequenced using both forward and reverse primers on an ABI-PRISM™ 310 Genetic Analyzer (Applied Biosystems Information, USA). Sequences were edited and aligned manually using BIOEDIT version 7.0.9.0 (Hall, 1999), the protein-coding region cyt *b* was translated into amino acids for confirmation of alignment, and sequences were deposited in GenBank under accession numbers (HM120761-HM120840).

2.4. Phylogenetic analysis

For phylogenetic analysis, we performed Bayesian inference (BI) by using the computer program MrBayes version 3.1.2 (Ronquist and Huelsenbeck, 2003). Three partitions (i.e. the three codon positions of the cyt *b* sequence) were applied to the data, and models of molecular evolution were assessed for each partition using MrModeltest version 2.3 (Nylander, 2004). We selected the best-fit model (SYM + I + G) for 1st codon position, (HKY + I + G) for 2nd codon position, and (GTR + G) for 3rd codon position by hLRT in MrModeltest version 2.3. Four Markov Chains Monte Carlo (MCMC) samplers were run for 2.2×10^6 generations. Two independent runs were performed to allow additional confirmation of the convergence of MCMC runs. Trees were sampled every 100 generations, providing 4.4×10^4 samples from the two runs. Analysis of the standard deviation of split frequencies between the two runs was used to determine that stationarity had been reached after 5×10^4 generations, which were typically discarded as burn-in, leaving 4.3×10^4 samples to estimate the consensus tree and the Bayesian posterior probabilities.

We used NETWORK version 4.5.1.0 to generate median-joining (MJ) networks of all individuals for both species (Bandelt et al., 1999) and compared the result with the resultant phylogenetic tree to visualize relationships among haplotypes within lineages. Given the relatively large numbers of haplotypes detected in our cyt *b* analyses, we used an initial star-contraction procedure (Forster et al., 2001) with a star connection limit of 2 to reduce the data set to facilitate data presentation and interpretation. Nodes in the MJ network were compared to collection locations to determine if some haplotypes were clustered geographically, with 95% haplotypes sampled from the same geographical regions. The number of haplotypes within and number of haplotypes unique to a particular collection site were calculated to test for correlation to both latitude and longitude using linear regression analysis.

2.5. Divergence times

Divergence times and evolutionary rates were estimated with a Bayesian MCMC method using the software Multidivtime (Thorne et al., 1998). The assumed topology was from the Bayesian phylogenetic analyses above. We followed the method of Rutschmann (2005) to estimate divergence time. The BI consensus tree topology and the sequence data were input into the software PAML (Yang, 1997) to estimate the model parameters. We used the program

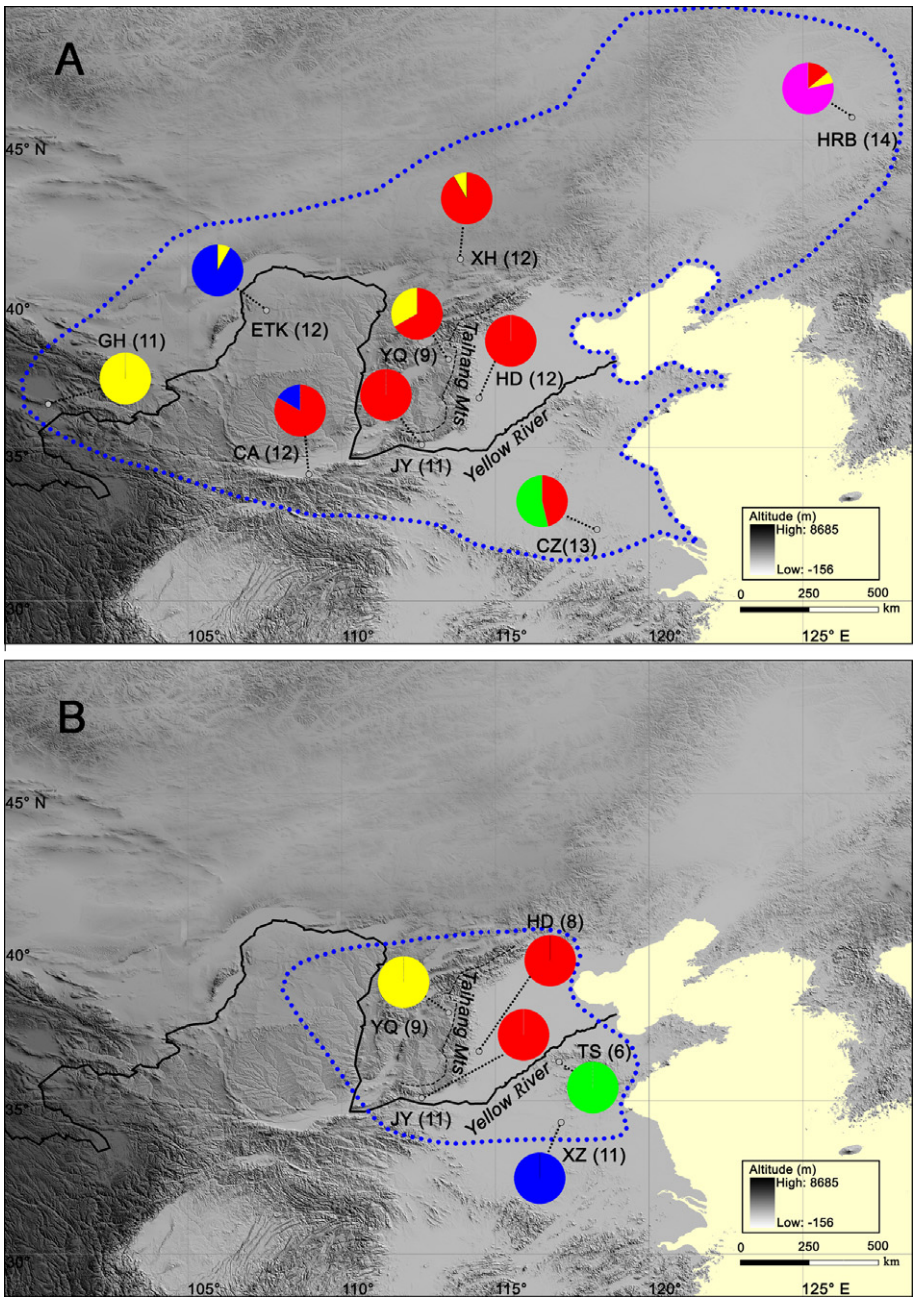

Fig. 1. Map of North China, showing the localities where lizards of *E. argus* (A) and *E. brenchleyi* (B) were collected. See text and Table 1 for population abbreviations. Numbers in parentheses are sample sizes. Small circles represent sampling sites, and pie charts represent haplotype group frequencies within each site. The blue, dotted lines outline the species distribution. Haplotype group color for *E. argus* is consistent with Fig. 3A, and haplotype group color for *E. brenchleyi* is consistent with Fig. 3B.

estbranches in the Multidivtime package to estimate the maximum likelihood of the branch lengths of the tree and the variance–covariance matrix. The mean of the prior distribution for the time separating the ingroup root from the present (rttm) was set to 39.15 million years (Myr), and the value, which is not a calibration point and does not have a major effect on posteriors, was an estimate based on the age of the split of *Eremias* and *Mesalina* because their divergence time was estimated to be 38.1–40.2 Myr with a mean of 39.15 Myr (Additional file 1, node 14 of Hipsley et al., 2009). The standard deviation of the prior distribution for the time separating the ingroup root from the present (rttmsd) was set at one-half of rttm. The mean and standard deviation of prior distribution for rate at root node (rtrate and rtratesd) both were set to 0.0059 substitutions per site per 1 Myr, with the rtrate value calculated by dividing the median distance between the ingroup root and the tips by rttm; the mean and standard deviation of prior for Brownian motion constant nu (brownmean and brownsd) both were set to 0.026, so that rttm × brownmean = 1, following recommendations accompanying the software. We set all the remaining parameters to the default values. We could use only one fossil calibration point in this study: the fossil of ancestor of *E. argus* from the Middle Pleistocene (0.438–0.548 Myr), found in Chinese fossil layers (Li et al., 2004). The fossil calibration point was assigned to the most recent common ancestor of *E. argus*. The Bayesian analysis was run for 2.2×10^6 generations, with a sample frequency of 100 after a burn-in of 1×10^5 generations.

Table 1
Descriptive statistics by sampling site for the two lizard species studied in this study. The following abbreviations are applied: PA, population abbreviation; NH, number of haplotypes; LSH, location-special haplotypes; MNBD, mean number of base-pair differences; ND, nucleotide diversity; *D*, Tajima's *D*; SSD, sum of square deviation between the observed and simulated mismatch distributions; MNM, mismatch number of modes; MV, mismatch variance.

Species	Collection site	PA	Latitude	Longitude	*n*	NH	LSH	MNBD	ND (π)	*D*	SSD	MNM	MV
E. argus					106	53				0.08	0.00372	2	
	Harbin, Heilongjiang	HRB	45.7	126.6	14	7	6	12	0.012	−1.40	0.05865	2	183.16
	Xinghe, Inner Mongolia	XH	41.1	113.9	12	4	4	5.6	0.005	−2.12**	0.26354***	3	114.79
	Etuoke, Inner Mongolia	ETK	39.5	107.5	12	8	8	8.6	0.008	−2.24***	0.01401	2	262.85
	Yangquan, Shanxi	YQ	37.9	113.6	9	6	6	14.9	0.014	1.53	0.10786	2	194.79
	Handan, Hebei	HD	36.6	114.5	12	9	9	13.2	0.013	0.94	0.05041*	2	87.55
	Gonghe, Qinghai	GH	36.4	100.5	11	4	3	0.7	0.001	−1.11	0.00155	1	0.66
	Jiyuan, Henan	JY	35.1	112.6	11	5	5	4.5	0.004	−1.54*	0.16481*	4	35.77
	Chang'an, Shaanxi	CA	34.0	108.9	12	6	6	16.4	0.016	0.24	0.78558***	4	250.82
	Chuzhou, Anhui	CZ	32.3	118.3	13	5	5	16.6	0.016	2.68	0.16575	2	214.30
E. brenchleyi					45	27				1.88	0.02605*	4	
	Yangquan, Shanxi	YQ	37.9	113.6	9	8	8	6.9	0.007	−0.70	0.02862	3	9.83
	Handan, Hebei	HD	36.6	114.5	8	3	3	9.2	0.009	−1.69*	0.55867***	3	213.14
	Taishan, Shandong	TS	36.3	117.1	6	6	6	14.1	0.013	−0.69	0.04877	8	88.35
	Jiyuan, Henan	JY	35.1	112.6	11	2	2	0.2	0.0002	−1.13	0.01756	1	0.15
	Xuzhou, Jiangsu	XZ	34.3	117.2	11	8	8	6.9	0.007	−1.63*	0.03556	3	51.11

* Significance at $P < 0.05$.
** Significance at $P < 0.01$.
*** Significance at $P < 0.001$.

2.6. Population genetic analyses

We used ARLEQUIN 3.11 (Schneider et al., 2000) to compute mean nucleotide diversity (π) within a collection site, mismatch distributions, and Tajima's *D* (Tajima, 1989a,b) for each sampling site (1000 replicates). These estimates were tested for a significant correlation with latitude using linear regression. Mismatch-distribution and Tajima's *D* values can potentially be used to indicate rapid demographic expansion. Mismatch-distribution tests were performed against the null model of sudden population expansion (Rogers and Harpending, 1992). Mismatch diversity is expected to follow a Poisson distribution (Slatkin and Hudson, 1991; Rogers and Harpending, 1992), and Tajima's *D* values are expected to be large negative values under demographic expansion. We calculated the time of possible population expansions from the relationship $\tau = 2ut$ (Rogers and Harpending, 1992), where τ measures the mode of the mismatch distribution, u measures the estimated mutation rate of the sequences, and t measures time in generations. The values of u for *E. argus* and *E. brenchleyi* were calculated as the mean for the estimations of evolutionary rates at internal nodes within the *E. argus* and *E. brenchleyi* clades, respectively. The generation time for *E. argus* and *E. brenchleyi* was estimated as 2 years based on approximate time at which animals become mature (Chen, 1994; Feng et al., 2004) and used to convert t into years. We used ARLEQUIN also to perform a two-level and a three-level hierarchical analysis of molecular variance (AMOVA) (Excoffier et al., 1992) [always with sampling location (population) as the smallest group] to investigate the partition of genetic variability. We performed a two-level AMOVA to test for structure among populations: within populations, and among populations (Φ_{ST}). Next, we performed a three-level AMOVA to test for structure among regions: within populations (Φ_{ST}), among populations within regions (Φ_{LR}), and between SYR and NYR (Φ_{RT}). The significance of Φ values was evaluated using 1000 nonparametric permutations (Weir and Cockerham, 1984). Furthermore, we computed the pairwise Φ_{ST} value for each combination of populations, which takes into account haplotype frequencies and the genetic distance between haplotypes in ARLEQUIN. The significance of Φ_{ST} values was evaluated using 1000 permutations of the data and was considered significant at $P = 0.05$. We performed a Mantel test to compare the pairwise population structure estimates to a matrix of geographical distance.

3. Results

3.1. Phylogeographical patterns

We obtained 1043 bp of the cyt *b* gene for *E. argus* with 53 haplotypes (Appendix A), and 1043 bp of the cyt *b* gene for *E. brenchleyi* with 27 haplotypes (Appendix B). The ratio of haplotypes relative to the total number of individuals sampled for each species was 0.50 for *E. argus* and 0.60 for *E. brenchleyi*. Mean nucleotide diversity per sampling location was 0.009 for *E. argus* and 0.007 for *E. brenchleyi*, but there was no significant difference between the two species ($F_{1,12} = 0.81$, $P = 0.38$). Relative to *E. brenchleyi*, *E. argus* had a similar high number of haplotypes and nucleotide diversity, and thus overall *E. argus* genetic diversity was similar to *E. brenchleyi*. For sampling locations of *E. argus*, genetic diversity was relatively low in GH. For sampling locations of *E. brenchleyi*, genetic diversity was relatively low in JY.

There was no significant difference in the number of haplotypes found in each sampling location between the two species ($F_{1,12} = 0.25$, $P = 0.63$; Table 1). The number of haplotypes per sampling location, the number of haplotypes that were unique to a particular sampling location and the mean number of base-pair differences within sampling location were correlated neither with latitude nor with longitude in both species (all $P > 0.17$).

Fig. 2 shows the Bayesian tree along with the Bayesian posterior probabilities. All haplotypes corresponding to *E. argus* formed a single well-supported clade designated as clade EA, while all haplotypes corresponding to *E. brenchleyi* formed another single well-supported clade designated as clade EB. Clade EA could be subdivided into two clades (EA I and EA II) that were mostly admixed in many local populations and had no geographical specificity. Clade EA I was further subdivided into four subclades (EA Ia, EA Ib, EA Ic and EA Id) that also had no geographical specificity. Clade EB was subdivided into two well-supported clades (EB I and EB II). Clade EB I included all haplotypes from three local populations (YQ, HD, and JY) in NYR, whereas clade EB II included all haplotypes from two local populations (XZ and TS) in SYR. The geographical division of these two clades coincided with the Yellow River (Figs. 1B and 2). There was a clear population-genetic structure within both clades. Clade EB I was further subdivided into three well-supported subclades (EB Ia, EB Ib and EB Ic) that formed two groups. Subclades EB Ia and EB Ib formed one group, including

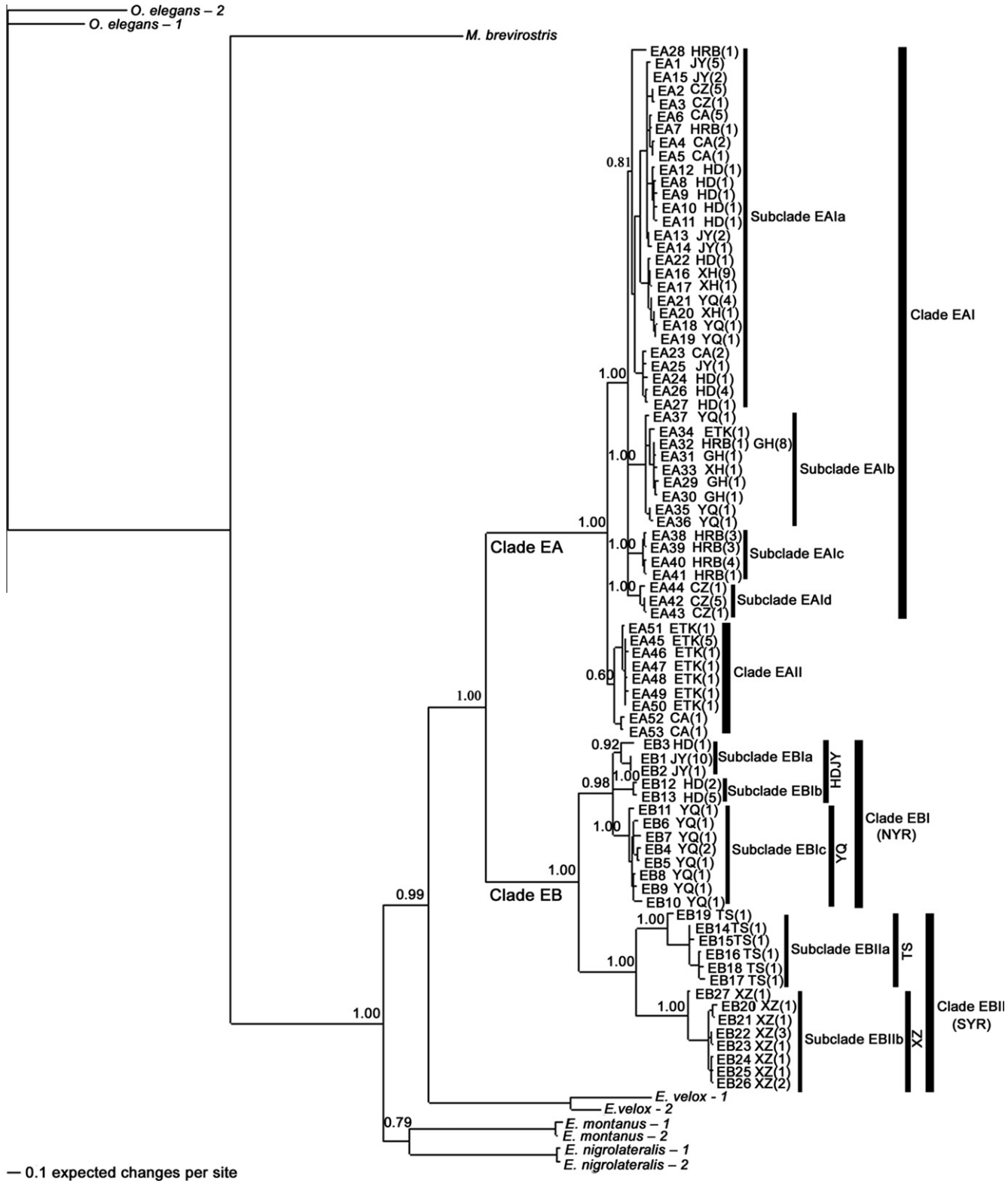

Fig. 2. The partitioned Bayesian phylogenetic tree based on cyt *b* haplotypes. Numbers above the branches are Bayesian posterior probabilities. Taxa are haplotypes; all haplotype designations are listed in Appendix C, followed by the sampling sites and numbers of individuals from each site having that haplotype [e.g. HRB(1)].

all haplotypes from two local populations [HD and JY (HDJY)] in the east of Taihang Mts; subclade EB Ic formed the other group, including all haplotypes from one local population (YQ) in the west of Taihang Mts. The geographical division of these two groups coincided with the Taihang Mts (Figs. 1B and 2). Clade EB II was further subdivided into two well-supported subclades (EB IIa and EB IIb). Subclade EB IIa included all haplotypes from one local population (TS), whereas subclade EB IIb included all haplotypes from one local population (XZ).

For *E. argus*, results of the median-joining network suggest little or no association between haplotypes and geography (Fig. 3A; Appendix A). We detected related haplotypes that form five groups

coinciding respectively with subclade EA Ia, EA Ib, EA Ic, EA Id, and clade EA II in the Bayesian phylogenetic tree (Fig. 2). Subclade EA Ia and EA Ib co-occurred in HRB, XH, and YQ. Subclade EA Ib and clade EA II co-occurred in ETK. Subclade EA Ia and clade EA II co-occurred in CA. Subclade EA Ia and EA Id co-occurred in CZ. Subclade EA Ia, EA Ib, and EA Ic co-occurred in HRB. The overall mismatch distribution of the set of cyt *b* haplotypes was bimodal indicating two distinct genetic groups (Table 1 and Fig. 3A).

For *E. brenchleyi*, however, we detected networks of related haplotypes that were clustered into two distinct areas (included: SYR and NYR) corresponding to clade EB I and EB II respectively in the Bayesian phylogenetic tree (Figs. 2 and 3B; Appendix B). We

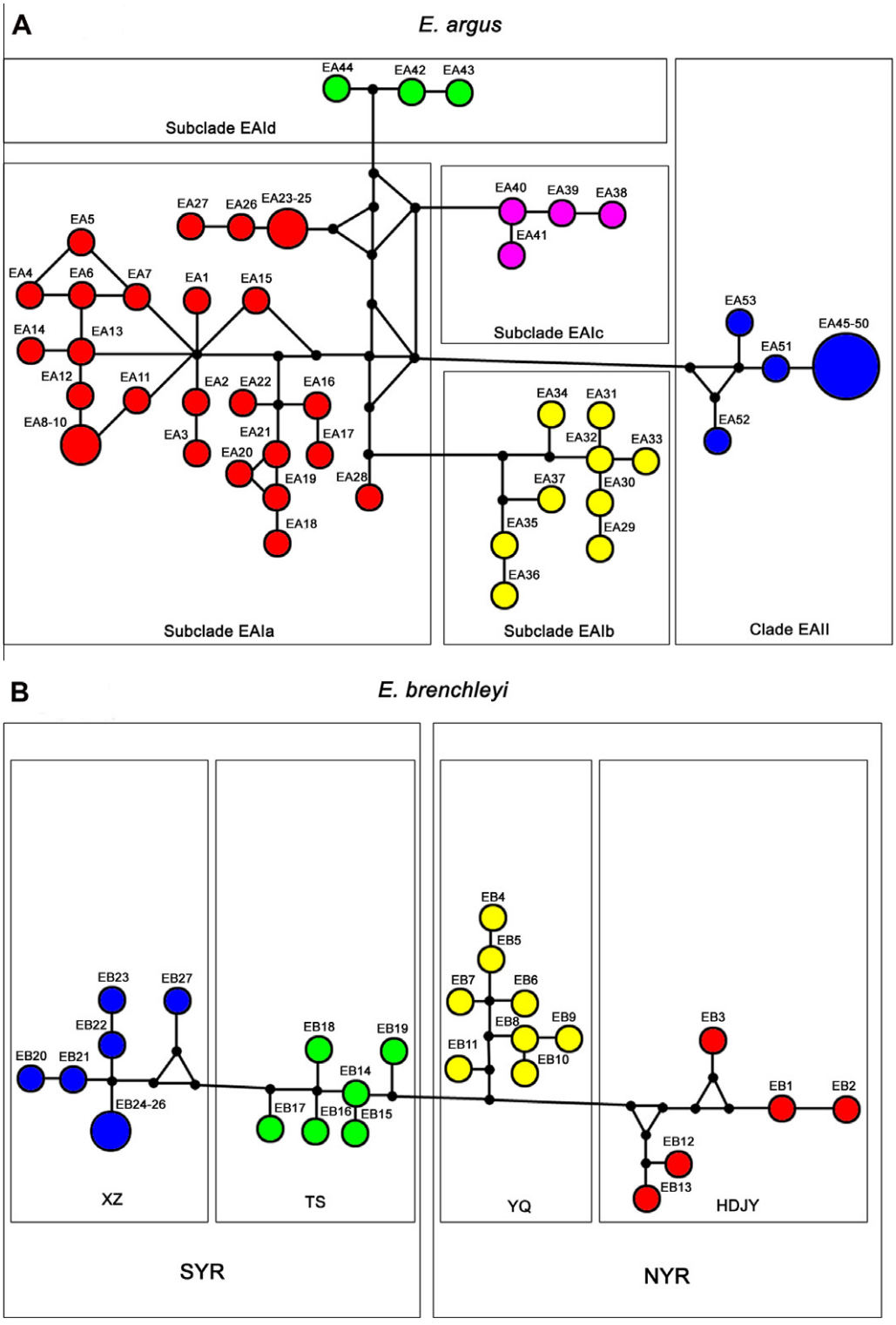

Fig. 3. Median-joining networks of mtDNA haplotypes at the cyt *b* gene in *E. argus* (A) and *E. brenchleyi* (B). Numbers adjacent to open circles (network nodes) refer to haplotypes listed in Appendices A and B. Haplotype group color for *E. argus* is consistent with Fig. 1A, and haplotype group color for *E. brenchleyi* is consistent with Fig. 1B. Small circles represent hypothesized (often ancestral) haplotypes that were required to connect existing haplotypes within the network. Data are presented using an initial star-contraction procedure with a star connection limit of 2.

further detected networks of related SYR haplotypes that were clustered into two distinct areas (i.e. TS and XZ), and detected networks of related NYR haplotypes that were clustered into two distinct areas (i.e. YQ, and HDJY). These four distinct areas (i.e. HDJY, YQ, TS, and XZ) therefore correspond to subclades EB Ia and EB Ib, subclade EB Ic, EB IIa, and EB IIb respectively in the Bayesian phylogenetic tree (Fig. 2). The mismatch distribution for the set of cyt *b* haplotypes was distinctly four-modal, indicating four distinct genetic groups (Table 1 and Fig. 3B).

3.2. Divergence times

Fig. 4 and Table 2 give posterior distribution of divergence times and evolutionary rates at each node as well as their 95% credibility intervals based on the phylogeny shown in Fig. 2. The divergence time of clade EA from clade EB (node 142) was dated to about 4.1 ± 1.2 million years ago (Ma) (with the 95% credibility interval ranging from about 2.4 to 6.8 Ma). The mean for divergence times within *E. argus* (clade EA) was about 0.1 Ma, younger than that for *E. brenchleyi* (clade EB), which was about 0.3 Ma ($F_{1,50} = 5.430$, $P = 0.023$). Moreover, the mean for the estimations of evolutionary rates at internal nodes within species was 0.02091 substitutions per site per 1 Myr for *E. argus*, and 0.02162 substitutions per site per 1 Myr for *E. brenchleyi*. For *E. argus*, clade EA I diverged from clade EA II at about 0.5 ± 0.03 Ma (with the 95% credibility interval ranging from about 0.4 to 0.5 Ma; node 141). The divergence time of subclade EA Ia, EA Ib, EA Ic, and EA Id was estimated to be about 0.4 ± 0.1 Ma (with the 95% credibility interval ranging from about 0.2 to 0.5 Ma; node 140). For *E. brenchleyi*, the divergence time of clade EB I and EB II was estimated to be about 2.2 ± 0.8 Ma (with the 95% credibility interval ranging from about 1.1 to 4.2 Ma; node 108). Within clade EB I, the divergence time of the HDJY clade (subclades EB Ia and EB Ib) from the YQ clade (subclade EB Ic) (node 107) was dated to about 0.7 ± 0.4 Ma (with the 95% credibility interval ranging from about 0.3 to 1.7 Ma). Within clade EB II, the divergence time of the TS clade (subclade EB IIa) from the XZ clade (subclade EB IIb) was dated to about 1.2 ± 0.5 Ma (with the 95% credibility interval ranging from about 0.5 to 2.5 Ma; node 98).

3.3. Population-genetic analysis

We analyzed *E. argus*, *E. brenchleyi*, and their populations to provide evidence for historical demographic changes through neutrality tests, goodness of fit to a simulated population expansion, and mismatch number of modes (Table 1). For *E. argus*, mismatch analysis did not indicate a rapid demographic expansion in most of the populations, where results within a sample site were mostly bimodal or multimodal and did not follow a Poisson distribution and had relatively high variance. However, for the GH population, a signal for demographic expansion was supported by lowest variance, one mismatch mode, and negative values of Tajima's *D*, and mismatch-distribution tests could not reject the null hypothesis of sudden population expansion. According to the value of τ (0.961), expansion of the GH population occurred about 0.02 Ma. For *E. brenchleyi*, mismatch analysis also did not indicate a rapid demographic expansion in all populations except in JY. JY had the lowest variance, one mode, and negative values of Tajima's *D*, and mismatch-distribution tests could not reject the null hypothesis of sudden population expansion. According to the value of τ (2.965), expansion of the JY population occurred about 0.07 Ma.

Results of AMOVA indicated the presence of geographic genetic structure within both species. For *E. argus*, when performing a two-level AMOVA to test for structure among populations, we detected high genetic structure ($\Phi_{ST} = 0.608$, $P < 0.001$). A small portion of the total genetic structure exists within populations, and the majority was among populations ($\Phi_{ST} = 0.608$, $P < 0.001$). When performing a three-level AMOVA to test for structure between SYR and NYR, we found that overall population structure was similar ($\Phi_{ST} = 0.614$, $P < 0.001$), with most genetic structure among populations occurring within a region ($\Phi_{LR} = 0.602$, $P < 0.001$). Little genetic structure was between SYR and NYR ($\Phi_{RT} = 0.030$, $P > 0.05$). For *E. brenchleyi*, when performing a two-level AMOVA to test for structure among populations, we detected relatively higher genetic structure ($\Phi_{ST} = 0.925$, $P < 0.001$). A small portion of the total genetic structure exists within populations, and the majority was among populations ($\Phi_{ST} = 0.925$, $P < 0.001$). When performing a three-level AMOVA to test for structure between SYR and NYR, we found that overall population structure was similar ($\Phi_{ST} = 0.944$, $P < 0.001$), but genetic structure among populations within a region and between SYR and NYR contained a nearly equal portion of genetic structure ($\Phi_{LR} = 0.851$, $P < 0.001$; $\Phi_{RT} = 0.625$, $P > 0.05$). Thus, relative to *E. argus*, *E. brenchleyi* had more significant geographical structuring.

For *E. argus*, pairwise area estimates of Φ_{ST} ranged from 0.132 to 0.919. All of the 36 pairwise Φ_{ST} values were statistically significant (Table 3). The results of the Mantel test between Φ_{ST} and geographical distance showed a weak relationship between population structure and distance ($R^2 = 0.18$, $P = 0.09$) (Fig. 5). For *E. brenchleyi*, pairwise area estimates of Φ_{ST} ranged from 0.772 to 0.972. All of the 10 pairwise Φ_{ST} values were statistically significant (Table 4). The results of the Mantel test between Φ_{ST} and geographical distance showed a statistically significant relationship between population structure and distance ($R^2 = 0.74$, $P = 0.01$) (Fig. 5).

4. Discussion

4.1. Genetic diversity and demographic history

The diversity indices of the two lizards studied herein are correlated neither with latitude nor with longitude, with the genetic diversity being almost homogeneous across their ranges. This finding is inconsistent with phylogeographic studies of widespread terrestrial species in North America and Europe, where they expanded from southern refugia at the end of the Pleistocene, thus exhibiting less geographically structured genetic diversity in the north (Hewitt, 1996, 1999, 2000). Our data show that the spatial pattern of genetic diversity seen in North American and European species cannot be observed in either *E. argus* or *E. brenchleyi*.

East Asia potentially hosts microclimatic zones capable of supporting a variety of habitats in relative stability (e.g. Qian and Ricklefs, 2000) because it is a mosaic of mountains lower than 2000 m and characterized by a relatively mild Pleistocene climate (Weaver et al., 1998; Ju et al., 2007). Multiple glacial refugia may have been available to East Asian species throughout their entire ranges (Li et al., 2009). One haplotype group of *E. argus* (clade EA II) formed at about 0.5 ± 0.03 Ma; four groups (subclade EA Ia, EA Ib, EA Ic, and EA Id) formed at about 0.4 ± 0.1 Ma. It is possible that the five haplotype groups diagnose five separate glacial refugia at the end of the Pleistocene for *E. argus*, according to the results reported in other similar studies (Hewitt, 1996, 2000; Zamudio and Savage, 2003). Genetic diversity in the GH population is low relative to other populations sampled. Very low variance, one mismatch mode, negative values of Tajima's *D*, and the mismatch-distribution test all support the inference of population expansion in GH. The GH population experienced a demographic change at about 0.02 Ma, probably because GH is on the Tibetan Plateau and may have been covered by ice sheets during the Quaternary (corresponding to Pleistocene–Holocene) glaciations (Li et al., 1991), and thus genetic diversity decreased with distance from glacial refugia during the interglacial. Of the four haplotype groups of

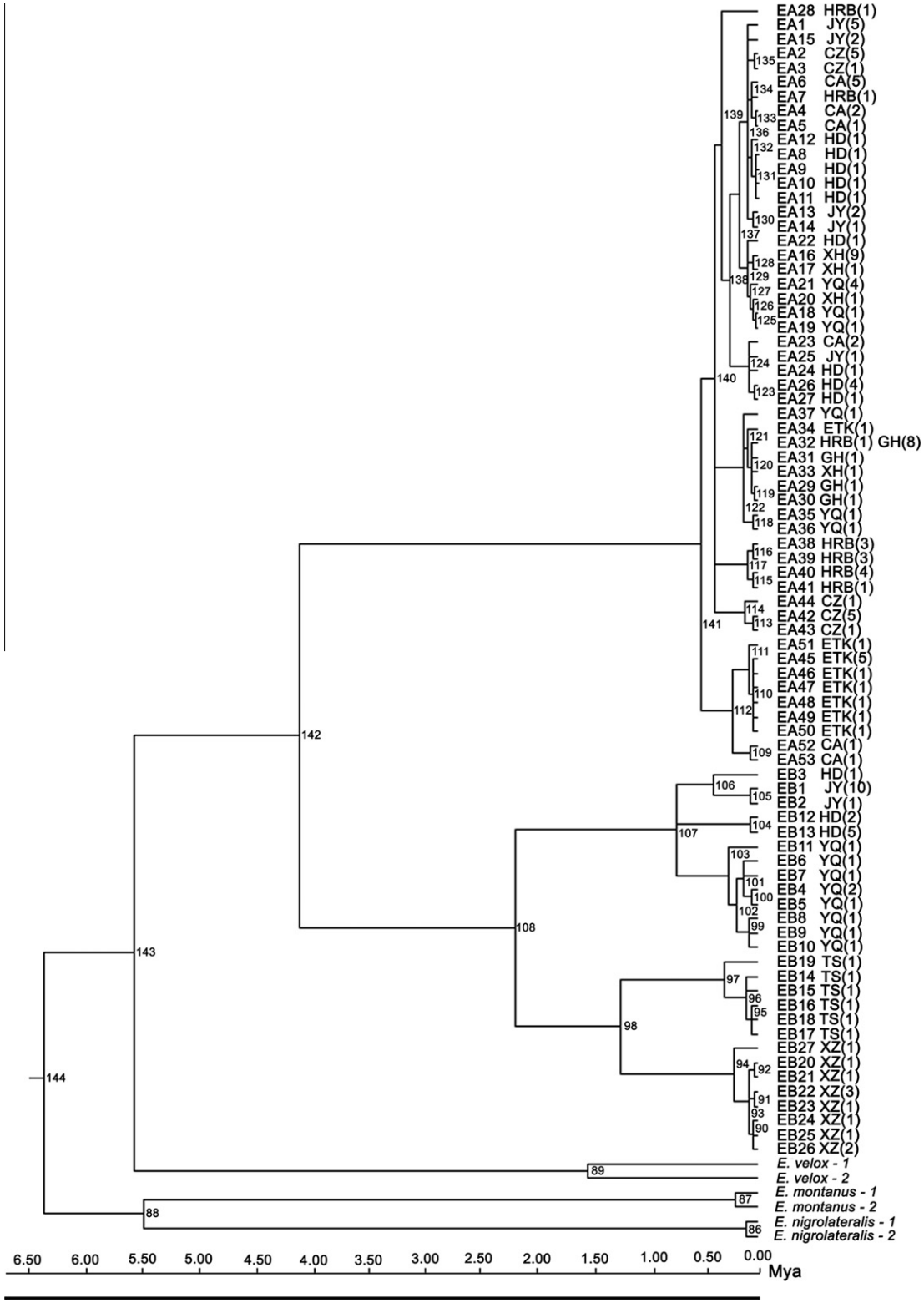

Fig. 4. Divergence events in *E. argus* and *E. brenchleyi* estimated from the cyt *b* fragment under a Bayesian relaxed clock. Branch lengths are proportional to divergence times. Node numbers are placed to the right of the corresponding node and correspond to node numbers in the Table 2. A time scale in millions of years is shown below. Taxa are haplotypes; all haplotype designations are listed in Appendix C, followed by the sampling sites and numbers of individuals from each site having that haplotype [e.g. HRB(1)].

E. brenchleyi, two (HDJY clade and YQ clade) formed at about 0.7 ± 0.4 Ma, and the other two (TS clade and XZ clade) at about 1.2 ± 0.5 Ma. It is possible that the four haplotype groups diagnose four separate glacial refugia at the end of the Pleistocene for *E. brenchleyi*. Genetic diversity in the JY population was low relative to all other populations sampled. Low variance, one mismatch mode, negative values of Tajima's *D*, and the mismatch-distribution test all supported population expansion in JY. From the value

Table 2
The posterior distribution of divergence times with 95% confidence intervals estimated by Bayesian molecular dating. The following abbreviations are applied: DT, divergence times; MDT, mean for divergence times; ER, evolutionary rates; MER, mean for evolutionary rates; SD, standard deviations; CI, the 95% credibility interval.

Species	Node	DT	SD for DT	CI for DT	ER	SD for ER	CI for ER	MDT	MER
	86	0.107	0.111	0.006–0.349	0.01933	0.00798	0.00584–0.03718		
	87	0.206	0.166	0.020–0.604	0.02001	0.00809	0.00642–0.03841		
	88	5.494	1.745	2.948–9.702	0.02264	0.00658	0.01176–0.03763		
	89	1.525	0.606	0.689–2.992	0.02446	0.00861	0.01139–0.04500		
E. brenchleyi								0.328	0.02162
	90	0.037	0.033	0.001–0.123	0.02372	0.00918	0.00959–0.04606		
	91	0.035	0.033	0.001–0.116	0.02372	0.00919	0.00949–0.04610		
	92	0.034	0.032	0.001–0.116	0.02373	0.00921	0.00955–0.04596		
	93	0.077	0.054	0.013–0.210	0.02373	0.00916	0.00961–0.04598		
	94	0.210	0.123	0.057–0.512	0.02367	0.00905	0.00965–0.04560		
	95	0.052	0.044	0.003–0.162	0.02259	0.00874	0.00865–0.04315		
	96	0.102	0.068	0.021–0.265	0.02256	0.00870	0.00860–0.04306		
	97	0.294	0.173	0.088–0.712	0.02248	0.00856	0.00881–0.04265		
	98	1.234	0.514	0.539–2.494	0.02390	0.00827	0.01132–0.04385		
	99	0.085	0.076	0.006–0.270	0.01946	0.00785	0.00590–0.03678		
	100	0.050	0.052	0.002–0.177	0.01947	0.00784	0.00585–0.03654		
	101	0.124	0.092	0.028–0.352	0.01949	0.00781	0.00600–0.03669		
	102	0.192	0.129	0.059–0.519	0.01949	0.00778	0.00609–0.03654		
	103	0.258	0.165	0.088–0.680	0.01953	0.00773	0.00612–0.03653		
	104	0.072	0.067	0.003–0.244	0.02011	0.00781	0.00672–0.03753		
	105	0.072	0.070	0.003–0.247	0.01962	0.00782	0.00612–0.03668		
	106	0.398	0.235	0.136–0.999	0.01988	0.00762	0.00683–0.03662		
	107	0.727	0.373	0.313–1.720	0.02017	0.00746	0.00752–0.03673		
	108	2.172	0.794	1.085–4.160	0.02339	0.00747	0.01165–0.04091		
E. argus								0.103	0.02091
	109	0.071	0.048	0.004–0.181	0.02099	0.00524	0.01157–0.03195		
	110	0.039	0.027	0.002–0.105	0.02096	0.00529	0.01149–0.03210		
	111	0.079	0.042	0.017–0.177	0.02096	0.00523	0.01158–0.03202		
	112	0.230	0.078	0.095–0.408	0.02107	0.00510	0.01192–0.03174		
	113	0.042	0.033	0.002–0.124	0.02105	0.00532	0.01168–0.03235		
	114	0.110	0.056	0.025–0.240	0.02108	0.00524	0.01181–0.03227		
	115	0.037	0.031	0.001–0.115	0.02113	0.00539	0.01162–0.03255		
	116	0.040	0.033	0.002–0.124	0.02111	0.00536	0.01159–0.03250		
	117	0.092	0.054	0.016–0.226	0.02114	0.00532	0.01175–0.03241		
	118	0.048	0.036	0.002–0.134	0.02098	0.00535	0.01148–0.03241		
	119	0.025	0.021	0.001–0.080	0.02099	0.00536	0.01149–0.03241		
	120	0.052	0.030	0.010–0.124	0.02100	0.00534	0.01156–0.03237		
	121	0.094	0.044	0.028–0.202	0.02101	0.00530	0.01165–0.03234		
	122	0.130	0.052	0.050–0.254	0.02100	0.00526	0.01170–0.03224		
	123	0.035	0.028	0.001–0.106	0.02079	0.00526	0.01143–0.03215		
	124	0.077	0.039	0.018–0.171	0.02080	0.00521	0.01157–0.03199		
	125	0.019	0.018	0.001–0.066	0.02073	0.00526	0.01130–0.03197		
	126	0.040	0.025	0.006–0.102	0.02073	0.00524	0.01142–0.03185		
	127	0.062	0.032	0.016–0.138	0.02073	0.00521	0.01145–0.03184		
	128	0.041	0.030	0.002–0.115	0.02072	0.00525	0.01138–0.03194		
	129	0.093	0.040	0.033–0.187	0.02074	0.00518	0.01151–0.03178		
	130	0.043	0.030	0.002–0.115	0.02073	0.00524	0.01139–0.03193		
	131	0.024	0.020	0.001–0.075	0.02074	0.00526	0.01131–0.03198		
	132	0.050	0.029	0.008–0.118	0.02075	0.00523	0.01139–0.03183		
	133	0.024	0.020	0.001–0.075	0.02074	0.00526	0.01135–0.03194		
	134	0.050	0.028	0.009–0.118	0.02074	0.00523	0.01138–0.03190		
	135	0.032	0.026	0.001–0.096	0.02075	0.00526	0.01135–0.03194		
	136	0.087	0.036	0.031–0.171	0.02075	0.00519	0.01147–0.03180		
	137	0.164	0.059	0.069–0.296	0.02081	0.00513	0.01166–0.03183		
	138	0.255	0.070	0.130–0.401	0.02093	0.00506	0.01193–0.03171		
	139	0.326	0.073	0.188–0.469	0.02106	0.00501	0.01213–0.03181		
	140	0.390	0.072	0.245–0.517	0.02116	0.00501	0.01218–0.03177		
	141	0.503	0.030	0.443–0.546	0.02124	0.00504	0.01216–0.03177		
	142	4.096	1.150	2.372–6.806	0.02414	0.00713	0.01289–0.04051		
	143	5.579	1.599	3.184–9.346	0.02299	0.00648	0.01222–0.03764		
	144	6.392	1.880	3.625–10.929	0.02299	0.00648	0.01222–0.03764		

of τ calculated by Arlequin soft, we estimated that the expansion of the JY population began at about 0.07 Ma. The JY population experienced a demographic change, probably for the same reason proposed above for *E. argus*.

The results of the Mantel test show that the genetic structure is significantly correlated with geographical distance ($R^2 = 0.74$, $P = 0.01$) in *E. brenchleyi*, but not in *E. argus* ($R^2 = 0.18$, $P = 0.09$). Thus, only *E. brenchleyi* shows conclusive evidence of isolation by distance (IBD). Isolation by distance based on a two-dimensional stepping-stone model of gene flow is the most realistic pattern (Kimura and Weiss, 1964; Slatkin, 1993). The range of genetic structure is narrower in *E. argus* (from 0.132 to 0.919) than in *E. brenchleyi* (from 0.772 to 0.972). Populations of both species almost have significant pairwise structure, indicating restricted gene flow among these populations. *Eremias brenchleyi* had more strongly restricted gene flow among the populations than did *E. argus*. Thus, *E. brenchleyi* had more significant geographical structuring of haplotype diversity than did *E. argus*.

Table 3
Eremias argus pairwise estimates of genetic structure (Φ_{ST}).

Population	HRB	XH	ETK	YQ	HD	GH	JY	CA	CZ
HRB	0.000								
XH	0.622+	0.000							
ETK	0.720+	0.805+	0.000						
YQ	0.484+	0.191+	0.698+	0.000					
HD	0.524+	0.453+	0.697+	0.352+	0.000				
GH	0.748+	0.881+	0.889+	0.687+	0.774+	0.000			
JY	0.673+	0.629+	0.820+	0.503+	0.259+	0.919+	0.000		
CA	0.517+	0.431+	0.638+	0.337+	0.144+	0.747+	0.132+	0.000	
CZ	0.476+	0.484+	0.686+	0.372+	0.279+	0.715+	0.376+	0.280+	0.000

+ Significance at $P < 0.05$.

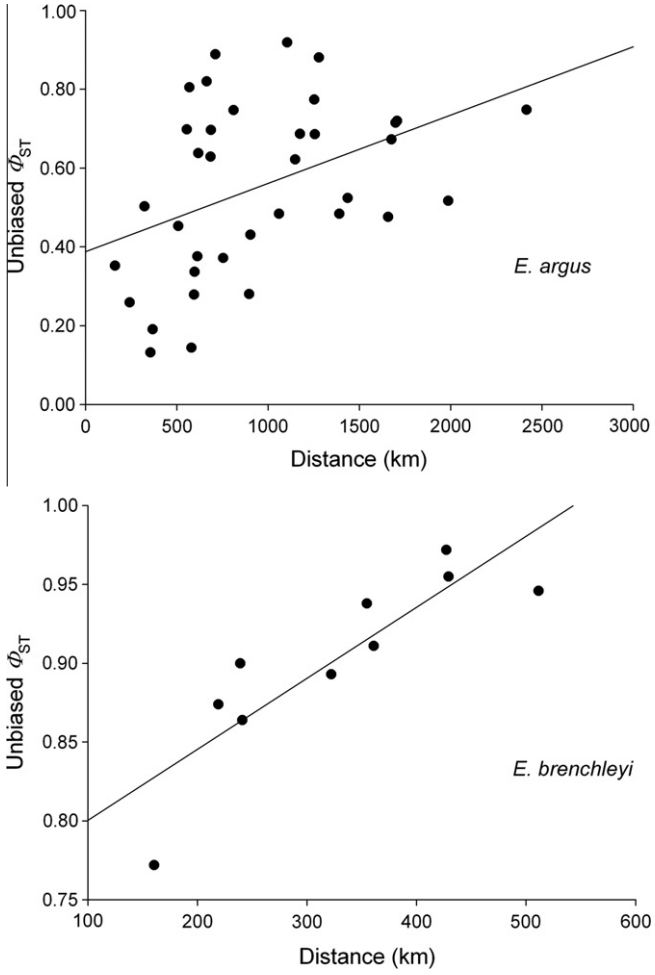

Fig. 5. Results of Mantel tests between pairwise geographical distance among sampling sites (kilometers), and pairwise Φ_{ST} estimates. Correlation coefficients and probabilities are given for each analysis in text.

Table 4
Eremias brenchleyi pairwise estimates of genetic structure (Φ_{ST}).

Population	YQ	HD	TS	JY	XZ
YQ	0.000				
HD	0.772+	0.000			
TS	0.911+	0.900+	0.000		
JY	0.893+	0.864+	0.955+	0.000	
XZ	0.946+	0.938+	0.874+	0.972+	0.000

+ Significance at $P < 0.05$.

4.2. Phylogeographical patterns

The Bayesian phylogenetic analysis strongly supported coalescence of mitochondrial haplotypes within *E. argus* and *E. brenchleyi*, consistent with their separate species status as reported by Wan et al. (2007). The divergence time of clade EA from clade EB was dated to about 4.1 ± 1.2 Ma (with the 95% credibility interval ranging from about 2.4 to 6.8 Ma), indicating a Late Miocene–Pliocene split between *E. argus* and *E. brenchleyi*. Climatic changes during Pleistocene glacial–interglacial cycles have played a dramatic role in shaping genetic diversity of these species, and global temperatures decreased significantly during Late Miocene–Pliocene (Kennett and Watkins, 1974; Guo et al., 2004).

Within the haplotype clade of *E. argus*, clade EA I diverged from clade EA II at about 0.5 ± 0.03 Ma (with the 95% credibility interval ranging from about 0.4 to 0.5 Ma). Considering that the two haplotype clades occurred together in many sampling sites and that there are no evident signs of isolation, we suppose that the subclades of *E. argus* can be attributed to the loss of intermediate haplotypes. Within *E. brenchleyi* (clade EB), there are two reciprocally well-supported haplotype clades that are the NYR clade (clade EB I) and the SYR clade (clade EB II), and their geographical separation occurs at the Yellow River (Fig. 1B). The Yellow River formed during the initial stage of the Early Pleistocene, i.e. about 1.6 Ma (Li et al., 1996; Zhang et al., 2003). The divergence time between the two lineages was estimated to be about 2.2 ± 0.8 Ma (with the 95% credibility interval ranging from about 1.1 to 4.2 Ma), and compared with the geographic record, *E. brenchleyi* may have been separated by the Yellow river into two lineages (NYR and SYR), with the lack of gene flow between NYR and SYR allowing them to the diverge genetically. Within clade EB I (the NYR lineage), there are two subclades of haplotypes corresponding to the HDJY lineage (subclades EB Ia and EB Ib) and the YQ lineage (subclade EB Ic). The geographical division of the two lineages coincides with the Taihang Mts (Fig. 1B). The Taihang Mts rose mainly during the Pleistocene–Holocene, and this mountain was uplifted to about 1100–1500 m (Wu et al., 1999). The divergence time of the HDJY lineage from the YQ lineage was dated to about 0.7 ± 0.4 Ma (with the 95% credibility interval ranging from about 0.3 to 1.7 Ma). Compared with the geographic record, the NYR lineage may have been separated by the Taihang Mts into two lineages (HDJY and TS). The divergence time of the TS clade (subclade EB IIa) from the XZ clade (subclade EB IIb) was dated to about 1.2 ± 0.5 Ma (with the 95% credibility interval ranging from 0.5 to 2.5 Ma), and we did not detect the mountain or river with which the geographical division of the two lineages coincided. We suppose that genetic divergence primarily results from the lack of gene flow between the two regions, probably because they are far enough from each other to result in isolation by distance.

Our results of median-joining network analysis revealed little or no association between haplotypes and geography in *E. argus*,

coinciding with results of the Bayesian phylogenetic analysis. Unlike *E. argus*, median-joining network analysis revealed geographic genetic structuring in *E. brenchleyi*, coinciding with results of the Bayesian phylogenetic analysis for *E. brenchleyi*. It is possible that the dispersal ability is greater in *E. argus* than in *E. brenchleyi*, so the Yellow River may not have served as a barrier for *E. argus* to disperse between SYR and NYR during the Yellow River zeroflow, and the Taihang Mts cannot act as a boundary between the lineages for *E. argus*. It has been reported for several species of animals that mountains or rivers act as barriers to gene flow. Zhang et al. (2008b) proposed that genetic structure of *Bufo pewzowi* was strongly affected by landscape, and they found three haplotype groups of this species in eastern Kazakhstan, Dzungaria and Tarim Basin, divided by the Tianshan and Dzungarian Alatau ranges. Several mountain ranges formed physical barriers between lineages in *Phrynocephalus vlangalii* (Jin et al., 2008). It is also found in *Scincella lateralis* that most lineages originated from population vicariance due to riverine barriers strengthened during the Plio-Pleistocene by a climate-induced coastal distribution (Jackson and Austin, 2009). Our data show that mountains or rivers may not always act as barriers to gene flow. In *E. argus*, for example, both the Yellow River and Taihang Mts may not have acted as important barriers to gene flow.

The total mismatch analysis of *E. argus* indicated two groups of haplotypes with no clear geographical correlation within the species. The overall mismatch analysis of *E. brenchleyi* indicated four major groups of haplotype, corresponding to the four phylogeographical units (Avise, 2000). This is concordant with results of the Bayesian phylogenetic analysis and median-joining network analysis. A rapid demographic expansion did not occur in most populations sampled for *E. argus* and *E. brenchleyi*, because results of mismatch analysis for these populations were either bimodal or multimodal and did not follow a Poisson distribution (Slatkin and Hudson, 1991; Rogers and Harpending, 1992; Harpending, 1994).

4.3. Population structure

Our AMOVA analysis indicated that among-population structure was high in *E. argus* and even higher in *E. brenchleyi*. This is consistent with many studies showing that geographic genetic structuring is strong for mtDNA variation in lizards (Clark et al., 1999; Stenson and Thorpe, 2003; Jin et al., 2008; Urquhart et al., 2009). Population structure has been negatively correlated with dispersal abilities (Bilton et al., 2001). Both species studied herein have significant population structure, but the finding that *E. brenchleyi* has stronger geographic genetic structuring than *E. argus* indicates that dispersal ability is lower in *E. brenchleyi* than in *E. argus*. This is consistent with our field observation that *E. argus* mainly inhabits plains and hills, while *E. brenchleyi* inhabits hills only. Our study provides evidence that genetic structure may differ between lizards that show differences in habitat preference and dispersal ability.

Our phylogeographical analysis for *E. brenchleyi* shows that there is significant geographic structuring of haplotype diversity, overall haplotypes are clustered into four distinct areas (included: XZ, TS, HDJY, and YQ), and no haplotype is shared among these four groups (Fig. 1B; Appendix B). We therefore suggest that the four groups should be regarded as four independent management units for *E. brenchleyi*. Comparatively, *E. argus* has generally lower amounts of population-genetic structure than does *E. brenchleyi*, so management units for *E. argus* may not occur. Thus, conservation strategies for coexisting lizards could be species specific. For *E. brenchleyi* and other similar species, we have to develop a more effective conservation strategy, and *in situ* protection measures should be taken because of their genetic uniqueness to preserve their genetic diversity.

Acknowledgments

The Provincial Forestry Departments of Anhui, Heilongjiang, Hebei, Henan, Inner Mongolia, Jiangsu, Qinghai, Shandong and Shanxi provided permits for collecting lizards. This work was supported by Grants from Chinese Ministry of Education (Project No. 20070319006) and Nanjing Normal University Innovative Team Project (Project No. 0319PM0902) to Ji's group. We thank Qi-Lei Hao, Li-Hua Li, Hong-Liang Lu, Yan-Fu Qu, Guo-Qiao Wang, Xue-Feng Xu, Jian-Long Zhang and Qun-Li Zhang for their assistance in collecting animals, and Long-Hui Lin for laboratory assistance.

Appendix A

Eremias argus haplotype frequency by population. Haplotype labels follow Figs. 2 and 4.

Haplotype number	HRB	XH	ETK	YQ	HD	GH	JY	CA	CZ
EA1							5		
EA2									5
EA3									1
EA4								2	
EA5								1	
EA6								5	
EA7	1								
EA8					1				
EA9					1				
EA10					1				
EA11					1				
EA12					1				
EA13							2		
EA14							1		
EA15							2		

Appendix A (*continued*)

Haplotype number	HRB	XH	ETK	YQ	HD	GH	JY	CA	CZ
EA16		9							
EA17		1							
EA18				1					
EA19				1					
EA20		1							
EA21				4					
EA22					1				
EA23								2	
EA24					1				
EA25							1		
EA26					4				
EA27					1				
EA28	1								
EA29						1			
EA30						1			
EA31						1			
EA32	1					8			
EA33		1							
EA34			1						
EA35				1					
EA36				1					
EA37				1					
EA38	3								
EA39	3								
EA40	4								
EA41	1								
EA42									5
EA43									1
EA44									1
EA45			5						
EA46			1						
EA47			1						
EA48			1						
EA49			1						
EA50			1						
EA51			1						
EA52								1	
EA53								1	

Appendix B

Eremias brenchleyi haplotype frequency by population. Haplotype labels follow Figs. 2 and 4.

Haplotype number	YQ	HD	TS	JY	XZ
EB1				10	
EB2				1	
EB3		1			
EB4	2				
EB5	1				
EB6	1				
EB7	1				
EB8	1				
EB9	1				
EB10	1				
EB11	1				
EB12		2			
EB13		5			
EB14			1		

(*continued on next page*)

Appendix B (*continued*)

Haplotype number	YQ	HD	TS	JY	XZ
EB15			1		
EB16			1		
EB17			1		
EB18			1		
EB19			1		
EB20					1
EB21					1
EB22					3
EB23					1
EB24					1
EB25					1
EB26					2
EB27					1

Appendix C

GenBank accession number for the lizard species in this study. The following abbreviation is applied: GAN, GenBank accession number.

Haplotype number	GAN	Haplotype number	GAN	Haplotype number	GAN
EA1	HM120763	EA31	HM120792	EB8	HM120824
EA2	HM120761	EA32	HM120791	EB9	HM120825
EA3	HM120762	EA33	HM120793	EB10	HM120826
EA4	HM120764	EA34	HM120794	EB11	HM120823
EA5	HM120765	EA35	HM120795	EB12	HM120817
EA6	HM120766	EA36	HM120796	EB13	HM120818
EA7	HM120767	EA37	HM120797	EB14	HM120827
EA8	HM120768	EA38	HM120798	EB15	HM120828
EA9	HM120769	EA39	HM120799	EB16	HM120829
EA10	HM120770	EA40	HM120800	EB17	HM120831
EA11	HM120771	EA41	HM120801	EB18	HM120830
EA12	HM120772	EA42	HM120802	EB19	HM120832
EA13	HM120773	EA43	HM120803	EB20	HM120833
EA14	HM120774	EA44	HM120804	EB21	HM120834
EA15	HM120775	EA45	HM120805	EB22	HM120835
EA16	HM120776	EA46	HM120806	EB23	HM120836
EA17	HM120777	EA47	HM120807	EB24	HM120837
EA18	HM120779	EA48	HM120808	EB25	HM120838
EA19	HM120780	EA49	HM120809	EB26	HM120839
EA20	HM120781	EA50	HM120810	EB27	HM120840
EA21	HM120782	EA51	HM120811	*E. velox – 1*	FJ416175
EA22	HM120778	EA52	HM120812	*E. velox – 2*	FJ416174
EA23	HM120783	EA53	HM120813	*E. montanus – 1*	FJ416299
EA24	HM120785	EB1	HM120814	*E. montanus – 2*	FJ416298
EA25	HM120784	EB2	HM120815	*E. nigrolateralis – 1*	FJ416291
EA26	HM120786	EB3	HM120816	*E. nigrolateralis – 2*	FJ416290
EA27	HM120787	EB4	HM120819	Outgroup	
EA28	HM120788	EB5	HM120820	*M. brevirostris*	FJ416173
EA29	HM120789	EB6	HM120821	*O. elegans – 1*	GQ142116
EA30	HM120790	EB7	HM120822	*O. elegans – 2*	FJ416172

References

Avise, J.C., 2000. Phylogeography: The History and Formation of Species. Harvard University Press, Cambridge.

Axelrod, D.I., Al-Shehbaz, I., Raven, P.H., 1996. History of the modern flora of China. In: Zhang, A.-L., Wu, S.G. (Eds.), Floristic Characteristics and Diversity of East Asian Plants. Higher Education Press, Beijing, pp. 43–55.

Bandelt, H.J., Forster, P., Röhl, A., 1999. Median-joining networks for inferring intraspecific phylogenies. Mol. Biol. Evol. 16, 37–48.

Bilton, D.T., Freeland, J.R., Okamura, B., 2001. Dispersal in freshwater invertebrates. Mol. Biol. Evol. 32, 159–181.

Bohonak, A.J., 1999. Dispersal, gene flow, and population structure. Quart. Rev. Biol. 74, 21–45.

Burbrink, F.T., Lawson, R., Slowinski, J.B., 2000. Mitochondrial DNA phylogeography of the polytypic North American rat snake (*Elaphe obsoleta*): a critique of the subspecies concept. Evolution 54, 2107–2118.

Byrne, M., 2008. Evidence for multiple refugia at different time scales during Pleistocene climatic oscillations in southern Australia inferred from phylogeography. Quat. Sci. Rev. 27, 2576–2585.

Chen, B.H., 1991. Lacertidae. In: Chen, B.H. (Ed.), The Amphibian and Reptilian Fauna of Anhui. Anhui Science and Technology Publishing House, Hefei, pp. 219–230.
Chen, S.-J., 1994. A preliminary observation on population structure and the severed tails regeneration of *Eremias argus*. Sichuan J. Zool. 13, 173–174.
Clark, A.M., Bowen, B.W., Branch, L.C., 1999. Effects of natural habitat fragmentation on an endemic scrub lizard (*Sceloporus woodi*): an historical perspective based on a mitochondrial DNA gene genealogy. Mol. Ecol. 8, 1093–1104.
Elderkin, C.L., Christian, A.D., Metcalfe-Smith, J.L., Berg, D.J., 2008. Population genetics and phylogeography of freshwater mussels in North America, *Elliptio dilatata* and *Actinonaias ligamentina* (Bivalvia: Unionidae). Mol. Ecol. 17, 2149–2163.
Excoffier, L., Smouse, P.E., Quattro, J.M., 1992. Analysis of molecular variance inferred from metric distances among DNA haplotypes: application to human mitochondrial DNA restriction data. Genetics 131, 479–491.
Feng, Z.-J., Sun, J.-M., Zhao, Y.-Y., Liu, C.-M., 2004. A preliminary study on ecology of *Eremias brenchleyi*. Sichuan J. Zool. 24, 359–366.
Forster, P., Torroni, A., Renfrew, C., Röhl, A., 2001. Phylogenetic star contraction applied to Asian and Papuan mtDNA evolution. Mol. Biol. Evol. 18, 1864–1881.
Fu, J.-Z., 1998. Toward the phylogeny of the family Lacertidae: implications from mitochondrial DNA 12S and 16S gene sequences (Reptilia: Squamata). Mol. Phylogenet. Evol. 9, 118–130.
Fu, J.-Z., 2000. Toward the phylogeny of the family Lacertidae: why 4708 base pairs of mtDNA sequences cannot draw the picture. Biol. J. Linn. Soc. 71, 203–217.
Gómez, A., Lunt, D.H., 2007. Refugia within refugia: patterns of phylogeographic concordance in the Iberian Peninsula. In: Weiss, S., Ferrand, N. (Eds.), Phylogeography of Southern European Refugia. Springer, Dordrecht, pp. 155–188.
Guo, Z.-T., Peng, S.-Z., Hao, Q.-Z., Biscaye, P.E., An, Z.-S., Liu, T.-S., 2004. Late Miocene–Pliocene development of Asian aridification as recorded in the Red-Earth Formation in northern China. Global Planet. Change 41, 135–145.
Hall, T.A., 1999. BIOEDIT: a user-friendly biological sequence alignment editor and analysis program for Windows 95/98/NT. Nucleic Acids Symp. Ser. 41, 95–98.
Hanski, I., 1998. Metapopulation dynamics. Nature 396, 41–49.
Harpending, H.C., 1994. Signature of ancient population growth in a low resolution mitochondrial DNA mismatch distribution. Hum. Biol. 66, 591–600.
Hewitt, G.M., 1996. Some genetic consequences of ice ages, and their role in divergence and speciation. Biol. J. Linn. Soc. 58, 247–276.
Hewitt, G.M., 1999. Post-glacial re-colonization of European biota. Biol. J. Linn. Soc. 68, 87–112.
Hewitt, G.M., 2000. The genetic legacy of the quaternary ice ages. Nature 405, 907–913.
Hewitt, G.M., 2004. Genetic consequences of climatic oscillations in the Quaternary. Philos. Trans. Roy. Soc. Lond. B 359, 183–195.
Hipsley, C.A., Himmelmann, L., Metzler, D., Müller, J., 2009. Integration of Bayesian molecular clock methods and fossil-based soft bounds reveals early Cenozoic origin of African lacertid lizards. BMC Evol. Biol. 9, 151.
Jackson, N.D., Austin, C.C., 2009. The combined effects of rivers and refugia generate extreme cryptic fragmentation within the common ground skink (*Scincella lateralis*). Evolution 64, 409–428.
Jin, Y.-T., Brown, R.P., Liu, N.-F., 2008. Cladogenesis and phylogeography of the lizard *Phrynocephalus vlangalii* (Agamidae) on the Tibetan Plateau. Mol. Ecol. 17, 1971–1982.
Ju, L.-X., Wang, H.-J., Jiang, D.-B., 2007. Simulation of the Last Glacial Maximum climate over East Asia with a regional climate model nested in a general circulation model. Paleogeogr. Paleoclimatol. Paleoecol. 248, 376–390.
Kennett, J.P., Watkins, N.D., 1974. Late Miocene–Early Pliocene paleomagnetic stratigraphy, paleoclimatology, and biostratigraphy in New Zealand. Geol. Soc. Am. Bull. 85, 1385–1398.
Kimura, M., Weiss, G.H., 1964. The stepping stone model of population structure and the decrease on genetic correlation with distance. Genetics 49, 561–576.
Li, B.-Y., Li, J.-J., Cui, Z.-J. (Eds.), 1991. Quaternary Glacial Distribution Map of Qinghai-Xizang (Tibet) Plateau 1: 3,000,000. Science Press, Beijing.
Li, J.-J., Fang, X.-M., Ma, H.-Z., Zhu, J.-J., Pan, B.-T., Chen, H.-L., 1996. Geomorphological evolution of Late Cenozoic River from upper Yellow River and the uplift of Qinghai-Tibetan Plateau on climatic changes. Sci. China Ser. D 26, 316–322.
Li, Y.-X., Xue, X.-X., Liu, H.-J., 2004. Fossil lizards of Qinling Mountains. Vertebr. Palasiatic. 42, 171–176.
Li, S.-H., Yeung, C.K.-L., Feinstein, J., Han, L.-X., Le, M.H., Wang, C.-X., Ding, P., 2009. Sailing through the Late Pleistocene: unusual historical demography of an East Asian endemic, the Chinese Hwamei (*Leucodioptron canorum canorum*), during the last glacial period. Mol. Ecol. 18, 622–633.
Meng, X.-F., Shi, M., Chen, X.-X., 2008. Population genetic structure of *Chilo suppressalis* (Walker) (Lepidoptera: Crambidae): strong subdivision in China inferred from microsatellite markers and mtDNA gene sequences. Mol. Ecol. 17, 2880–2897.
Nylander, J.A.A., 2004. MRMODELTEST version 2.1. Computer Program Distributed by the Author. Uppsala University, Uppsala.
Page, R.D.M., 1994. Maps between trees and cladistic analysis of historical associations among genes, organisms, and areas. Syst. Biol. 43, 58–77.
Palumbi, S.R., 1996. Nucleic acids II: the polymerase chain reaction. In: Hillis, D.M., Moritz, C., Mable, B.K. (Eds.), Molecular Systematics, second ed. Sinauer Associates, Inc., Massachusetts, pp. 205–247.
Qian, H., Ricklefs, R.E., 2000. Large-scale processes and the Asian bias in temperate plant species diversity. Nature 407, 180–182.
Rogers, A.R., Harpending, H., 1992. Population growth makes waves in the distribution of pairwise genetic differences. Mol. Biol. Evol. 9, 552–569.
Ronquist, F., Huelsenbeck, J.P., 2003. MrBayes 3: Bayesian phylogenetic inference under mixed models. Bioinformatics 19, 1572–1574.
Rutschmann, F., 2005. Bayesian Molecular Dating using PAML/Multidivtime. A Step-by-step Manual. University of Zurich, Switzerland. <http://www.plant.ch>.
Schneider, S.H., Kueffer, J., Roessli, D., Excoffier, L., 2000. ARLEQUIN: A Software for Population Genetic Data Analysis, Version 2.0. Genetics and Biometry Laboratory, Department of Antropology, University of Geneva, Switzerland.
Slatkin, M., 1993. Isolation by distance in equilibrium and nonequilibrium populations. Evolution 47, 264–279.
Slatkin, M., Hudson, R.R., 1991. Pairwise comparisons of mitochondrial DNA sequences in stable and exponentially growing populations. Genetics 129, 555–562.
Stenson, A.G., Thorpe, R.S., 2003. Phylogeny, paraphyly and ecological adaptation of the colour and pattern in the *Anolis roquet* complex on Martinique. Mol. Ecol. 12, 117–132.
Tajima, F., 1989a. Statistical method for testing the neutral mutation hypothesis. Genetics 123, 585–595.
Tajima, F., 1989b. The effects of change in population size on DNA polymorphism. Genetics 123, 597–601.
Thomas, C.D., 2000. Dispersal and extinction in fragmented landscapes. Proc. Roy. Soc. Lond. B 267, 139–145.
Thorne, J.L., Kishino, H., Painter, I.S., 1998. Estimating the rate of evolution of the rate of molecular evolution. Mol. Biol. Evol. 15, 1647–1657.
Urquhart, J., Wang, Y.-Z., Fu, J.-Z., 2009. Historical vicariance and male-mediated gene flow in the toad-headed lizards *Phrynocephalus przewalskii*. Mol. Ecol. 18, 3714–3729.
Wan, L.-X., Sun, S.-H., Jin, Y.-T., Yan, Y.-F., Liu, N.-F., 2007. Molecular phylogeography of the Chinese lacertids of the genus *Eremias* (Lacertidae) based on 16S rRNA mitochondrial DNA sequences. Amphibia–Reptilia 28, 33–41.
Wares, J.P., Turner, T.F., 2003. Phylogeography and diversification in aquatic mollusks. In: Lydeard, C., Lindberg, D.R. (Eds.), Molecular Systematics and Phylogeography of Mollusks. Smithsonian Books, Washington, DC, pp. 229–269.
Weaver, A.J., Eby, M., Fanning, A.F., Wiebe, E.C., 1998. Simulated influence of carbon dioxide, orbital forcing and ice sheets on the climate of the Last Glacial Maximum. Nature 394, 847–853.
Weir, B.S., Cockerham, C.C., 1984. Estimating *F*-statistics for the analysis of population structure. Evolution 38, 1358–1370.
Williams, M.A.J., Dunkerley, D.L., de Deckker, P., Kershaw, A.P., Chappel, J., 1998. Quaternary Environments. Arnold, London.
Wu, C., Zhang, X.-Q., Ma, Y.-H., 1999. The Taihang and Yan mountains rose mainly in Quaternary. N. China Earthq. Sci. 17, 1–7.
Yang, Z.-H., 1997. PAML: a program package for phylogenetic analysis by maximum likelihood. Comput. Appl. Biosci. 13, 555–556.
Zamudio, K.R., Savage, W.K., 2003. Historical isolation, range expansion, and secondary contact of two highly divergent mitochondrial lineages in spotted salamanders (*Ambystoma maculatum*). Evolution 57, 1631–1652.
Zhang, R.-Z., Zheng, C.-L., 1981. The geographical distribution of mammals and the evolution of mammalian fauna in Qinghai-Xizang Plateau. In: Geological and Ecological Studies of Qinghai-Xizang Plateau. Science Press, Beijing, pp. 1005–1012.
Zhang, Z.-Y., Yu, Q.-W., Zhang, K.-X., Gu, Y.-S., Xiang, S.-Y., 2003. Geomorphological evolution of Quaternary River from upper Yellow River and geomorphological evolution investigation for 1:250000 scale geological mapping in Qinghai-Tibet plateau. J. China Univ. Geosci. 28, 621–633.
Zhang, Q., Chiang, T.Y., George, M., Liu, J.-Q., Abbott, R.J., 2005. Phylogeography of the Qinghai-Tibetan Plateau endemic *Juniperus przewalskii* (Cupressaceae) inferred from chloroplast DNA sequence variation. Mol. Ecol. 14, 3513–3524.
Zhang, H., Yan, J., Zhang, G.-Q., Zhou, K.-Y., 2008a. Phylogeography and demographic history of Chinese black-spotted frog populations (*Pelophylax nigromaculata*): evidence for independent refugia expansion and secondary contact. BMC Evol. Biol. 8, 21.
Zhang, Y.-J., Stöck, M., Zhang, P., Wang, X.-L., Zhou, H., Qu, L.-H., 2008b. Phylogeography of a widespread terrestrial vertebrate in a barely-studied Palearctic region: green toads (*Bufo viridis* subgroup) indicate glacial refugia in Eastern Central Asia. Genetica 134, 353–365.
Zhao, K.-T., 1999. Lacertidae. In: Zhao, E.-M., Zhao, K.-T., Zhou, K.-Y. (Eds.), Fauna Sinica, Reptilia (Squamata: Lacertilia), Vol. 2. Science Press, Beijing, pp. 219–242.